V European Conference on Computational Fluid Dynamics
ECCOMAS CFD 2010
J. C. F. Pereira and A. Sequeira (Eds)
Lisbon, Portugal,14-17 June 2010

A NOVEL ENERGETICS MODEL FOR EXAMINING FLAPPING FLIGHT IN NATURE AND ENGINEERING

Hesam Salehipour* **and David J. Willis***

*University of Massachusetts Lowell, Mechanical Engineering Department
1 University Ave, Lowell, MA, 01854, USA
e-mail: hesam_salehipour@student.uml.edu, david_willis@uml.edu

Key words: Energetics, Numerical model, Flapping flight, Wing-beat, Kinematics, Micro Air Vehicle (MAV)

Abstract. *Several methods exist for estimating flapping flight power requirements; however, many of these approaches use aerodynamic models that ignore the relationship between wing kinematics (eg. flapping amplitude and frequency) and power requirements. This relationship may be critical for improving the performance of flapping wing micro aerial vehicle designs. We have proposed an energetics model based on an optimal vorticity, wake-only solution method for predicting the aerodynamics of flight. The energetics model is composed of (1) a cost intensive offline, (2) a moderate cost intermediate and (3) an efficient online component. The main components of our model as well as the latest viscous-inviscid modification are explained briefly in this paper. The energetics model is applied to a small budgerigar (Melopsittacus undulatus), to demonstrate suitability of the analysis for biological studies. The results show promising agreement with available experimental measurements. We also use the energetics model to investigate parameter choice and sensitivity of a flapping wing micro air vehicle of similar size to the budgerigar.*

1 INTRODUCTION

1.1 The Relationship between Flight Kinematics and Flight Energetics

Natural flyers modulate flapping motions in response to different flight conditions and demands. For example, efficient climbing flight may necessitate different flapping amplitude and/or frequency choices than level flight. Understanding kinematics preferences is the first step in replicating flapping propulsion in micro aerial vehicle (MAV) applications. It is likely that animals exploit kinematics that lower flight energy or extend range. We hypothesize that natural flight strategies and parameter choices are nearly optimal and will have low sensitivity to parameter variation. We postulate this because of the links observed in nature between general flapping kinematics and flight condition.

Directly exploring the flapping design space is impractical. For compliant wings, the possible combination of flapping motions, structural parameters and geometry parameters is infinite. Zeroing in on a local optimum in the design space may work for certain flight conditions, but the results of such a study would not necessarily generalize to other designs and flight conditions. Also, using higher fidelity representations of the geometry and/or physics is infeasible for design space exploration. For example, designing a flapping wing with variable local angle of attack, flapping amplitude and frequency, introduces a massive, multi-dimensional optimization problem. In this paper, we use an aerodynamic model based only on the wake behind the flapping wing. Reducing the aerodynamics problem to a wake-only analysis allows us to ignore many of the complexities related to the wing geometry and focus directly on the fluid dynamics of flapping flight – namely the distribution of kinetic energy that is deposited as vorticity in the trailing wake that is necessary to generate the forces on the wing.

1.2 Micro Air Vehicle (MAV) – Biological Inspiration

Biological-inspiration [1] is a focus in much current Micro Air Vehicle (MAV) design. Although engineered flapping wing vehicles fly, it is not clear how efficient they are. Also, despite the plethora of natural flight examples, it is unclear which parameters are related to minimizing flight power and which are related to constraints on the biological system. Understanding how flight kinematics are related to flight power is therefore critical for effective conceptual and preliminary design of MAVs.

In the energetics model, a low-fidelity wake-only computational aerodynamics method is coupled with a design space reduction algorithm and the resulting energetics model is used to evaluate the MAV and natural flyers. This model is comprised of three components, an *offline*, an *intermediate*, and an *online* code. The *offline* portion of the computation constructs a database of the optimal aerodynamics for all possible flapping kinematics. The *intermediate* code is used to construct response surfaces for each of the flapping parameters as functions of the lift and thrust coefficient combinations. In the *online* computation the force balance is performed and the kinematics of optimal energetics flight are determined as a function of forward flight speed.

1.3 Historical Context: Past Research in Flight Energetics

Over the past four decades, several computational models for evaluating flight energetics have been proposed [2]. Those models proposed by Pennycuick [3, 4] and Rayner [5] have become the *standard* first order analysis tools and are still used for flight power prediction [6]. Pennycuick's computer code, *Flight* [7], is an example of one such analysis tool. At the core of each of these methods is a low-order, quasi-steady, aerodynamic analysis. In addition, ad-hoc approximations are employed to estimate the total power. Pennycuick's model is advantageous due to its simplicity and ease of use. Although the method predicts the energetics of flight efficiently, it ignores the fundamental unsteady aerodynamics and kinematics. Our novel model [8], is the first energetics model capable of consistently predicting correlations between flight power requirements and wing-beat kinematics. In this paper, we illustrate our energetics model [8]. Following an introduction to the theory, the model's capabilities are explored in a rigorous energetics analysis.

2 ENERGETICS MODEL THEORY

In our energetics model [8] the complex motion of a flapping wing is simplified by assuming a simple harmonic flapping motions about a centerbody hinge. This simplified flapping geometry is analysed using a wake-only method [9]. In the energetics model, the wake-only method is considered as a black-box [10].

2.1 Wake-Only Method

The wake-only method is used to find the minimum circulation distribution for a prescribed wake geometry (figure 1) using a vortex lattice discretization of the wake [9]. In the *offline* portion of our energetics model, the minimum power wake circulation (or vorticity) distribution is computed for all possible wake shapes (flapping frequency and amplitude pairs) using this wake-only aerodynamics tool. In addition, this energetics evaluation is performed for a large array of possible lift and thrust coefficients (C_L and C_T values).

We implemented the wake-only method as described by Hall et al. [9], with several modifications [8, 10]. These modifications include, (a) no stall penalty, (b) an induced velocity/drag computation, (c) a viscous drag computation and (d) viscous-inviscid decoupled independent calculations [8, 10]. The viscous-inviscid decoupling enabled more accurate representation of varying Reynolds number (Re) and aspect ratio (AR).

2.2 Proposed Energetics Flapping Model

The detailed data flow as well as the pseudo-code for different components of our model are described in Salehipour and Willis [8]. For this paper, we illustrate the general concept of the energetics model in figure 2. During the offline component, a large collection of wake-only computations are performed corresponding to different C_L, C_T , $Amplitude$ and $Frequency$ inputs. In the present model, $60C_L \times 130C_T \times 33freq \times 57Amplitudes \approx$

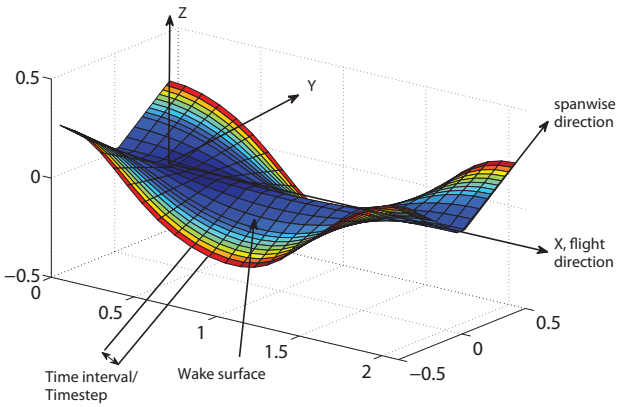

Figure 1: The coordinate system and nomenclature for the wake-only method. The wake geometry used is simply the fixed in space trace of the trailing edge of the wing.

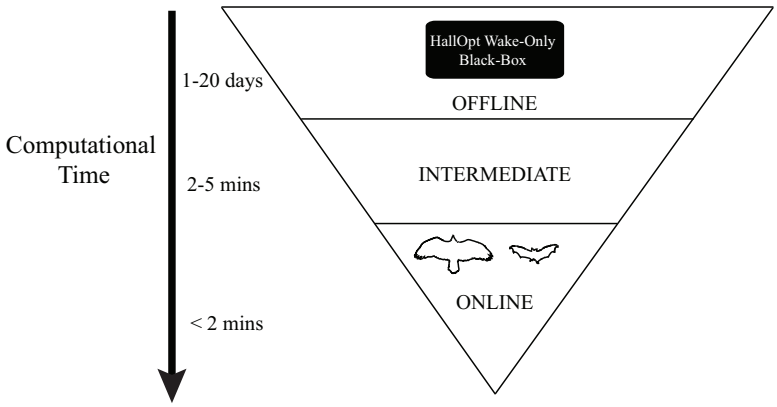

Figure 2: The energetics model components and their relative computational time.

$14,500,000$ individual wakes are analysed to form the offline database. This energetics database is only computed once and represents approximately 6-months of (single) processor time. Following the offline portion, an *intermediate* code is used to reduce the data (based on a minimum power requirement) and assemble response surfaces (figure 3). Finally vehicle parameters are introduced during the *online* component. During the *online* component a force balance is imposed (lift equals weight and thrust equals drag) at each of the desired flight conditions (forward flight speed and climb/descent angle). For each individual animal or vehicle, the only required parameters are mass (M), wing span (b), aspect ratio (AR) and flight speed range. Each energetics evaluation (*intermediate* and *online*) takes less than five minutes. The response surfaces in figure 3 correspond to the minimum power parameter dependencies as a function of the prescribed lift and thrust coefficients. These parameters include frequency and amplitude as well as offline outputs (individual and total drag and power components).

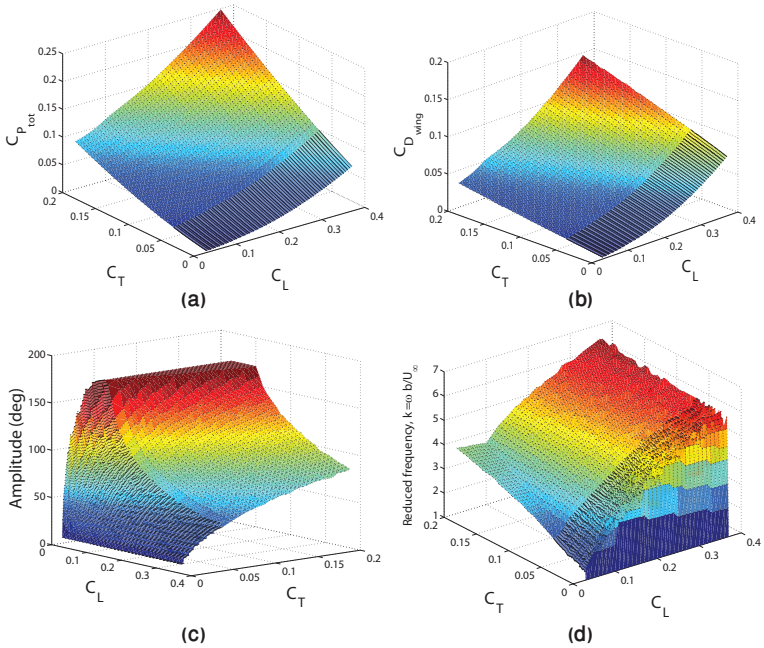

Figure 3: Flapping parameter response surfaces for a range of C_L and C_T non-dimensionalized by $b = 1$, (a) $C_{P,min}$, total minimum power coefficient consists of induced, viscous, inertial and parasite power, (b) The wing-only total drag coefficient corresponding to $C_{P,min}$, (c) Flapping amplitude corresponding to $C_{P,min}$ and (d) Reduced frequency corresponding to $C_{P,min}$.

2.2.1 Viscous-Inviscid Decoupled Energetics Model

The viscous contribution is inherently Reynolds number dependent. One limitation of our preliminary model [8] was that the whole offline database was built only using a single Reynolds number, Re, (one set of drag coefficients (C_{d0} and C_{d2})). Considering the computational cost of offline computations, it was impractical to build databases for each Reynolds number. In our newly proposed viscous-inviscid model (V-I model), these inadequacies are avoided by decoupling the viscous and inviscid computations. This approach has been implemented and validated [10].

In table 1, all of the different components that comprise the total mechanical power are shown. Their mathematical relationship is also given. The viscous and inviscid powers are expressed as functions of the optimal circulation distribution (Γ) over the wake surface, [8, 10].

2.2.2 Energetics Model Capabilities

The energetics model is ideal for both the analysis of biological flyers as well as the preliminary design of micro aerial vehicles. Besides delivering promising predictions [8],

Power	Mathematical Expression	Energetics Model
Total mechanical power	$P_{tot} = P_{ind} + P_{visc} + P_{par} + P_{iner}$	online
Induced power [9, 8]	$P_{ind} = -\frac{\rho}{2T}\iint_W \Gamma\omega \cdot n dA$	offline
Viscous power [9, 8]	$P_{visc} = \left(\frac{4C_{d2}}{\bar{c}}\right) P_1 + (\bar{c}C_{d0})P_2$ $P_1 = \frac{\rho}{2T}\iint_W (\Gamma - \Gamma_0)^2 dA$ $P_2 = \frac{\rho}{2T}\iint_W U^2 \cdot \left(\frac{ds}{dx}\right)^2 dA$	intermediate offline offline
Parasite power [11]	$P_{par} = \frac{1}{2}\rho S_b C_{D,par} V^3$ $S_b = 0.00813 M^{0.666}$	online
Inertial power [8, 10]	$P_{iner} = \frac{2\alpha}{1-\tau} I_{up} \pi^2 A^2 f^3$	intermediate

Table 1: Mathematical expressions for different components of total power including their implementation location in the energetics model

our model is fast (less than 5 minutes per energetics evaluation) and is simple to use. In addition, the method is capable of easily analyzing ascending and descending flight.

One additional feature of our model is the ability to study different Kinematic Constraint modes (KC modes). We have implemented four different KC modes that enable us to constrain flapping frequency or flapping amplitude. These four KC modes are namely:

1. KC mode 1: Amplitude and frequency are determined based on minimum power flight.

2. KC mode 2: Amplitude is user prescribed but frequency is determined based on minimum power flight.

3. KC mode 3: Frequency is user prescribed but amplitude is determined based on minimum power flight.

4. KC mode 4: Amplitude and frequency are both user prescribed.

We have used KC mode 1, 2 and 3 for a variety of cases in the present parametric study.

3 RESULTS AND DISCUSSION

The energetics model results for a small budgerigar, *Melopsittacus undulatus*, are presented here. In addition to analysing biological trends in animals, we also illustrate how this model can be applied to preliminary exploration of the bio-inspired micro air vehicle (MAV) design space.

Measure	symbol	units	*Melopsittacus undulatus*
Body mass	M	kg	0.045
Span	b	m	0.2915
Wing area	A	m^2	0.0111146
Aspect ratio	AR	–	7.65
Span ratio	R	–	0.5 [14]
Downstroke ratio	τ	–	0.5
Upstroke impact factor	α	–	0.3
Body drag coefficient	$C_{D,body}$	–	0.05[12]

Table 2: Morphological data for a budgerigar used for calculating flight energetics.

3.1 Biological Flapper: Budgerigar *Melopsittacus undulatus*

In this section we present the flight energetics results for a budgerigar. The numerical predictions for optimal power are compared with *in vitro* measurements of the mechanical power by Askew and Ellerby [12]. Also wind-tunnel data of budgerigar flight tests [13] are used to validate the energetics predictions of the minimum power frequency at different flight speeds [1]. Table 2 shows the morphological data for this small bird [2]. Figure 4 illustrates the computed and experimentally observed relationships between kinematics and energetics. The variation of mechanical power, amplitude and frequency with flight speed ($5m/s$ to $15m/s$) is shown. Good agreement with the power predictions of Askew are obtained when using the proposed value of $C_{D,body} = 0.05$ [12]. In [12] it was already shown that traditional energetics models provide promising power predictions; however, our model is unique since it also predicts the correlation between the predicted power and wing-beat kinematics. The upper and lower bounds of the amplitude and frequency correspond to the range of parameter values that are within 10% of the minimum power result. These bounds provide a first order indication of the sensitivity of flight energetics to wing kinematics. For the case shown in figure 4 (b) and (c), it is clear that a broad range of wing-beat kinematics are included in the 10% power bound. As such, our energetics model confirms the expected lower sensitivity of flight energetics to kinematics parameters as well as illustrating that animals do tend to choose kinematics that exploit efficient flight.

Kinematics parameters associated with ascending flight can also be compared using our model. Similar to cruise energetics, the power, amplitude and frequency associated with a budgerigar flying at a $\theta = 15^\circ$ climb angle is shown in figure 5. By comparing the climb results (figure 5) to level flight (figure 4), we observe that the power required for climb is, as expected, greater than level flight. Similarly, the flapping amplitude in climb is almost double that of level flight. The amplitude increase correlates with observations

[1] Tobalske and Dial [13] used $N = 8$ budgerigars with a mean body mass of 34.5 ± 0.5 g, ranging $29.0 - 40.0$ g. For the present study, the mean frequency data are therefore taken, although budgerigar's mass differ slightly from the bird used to collect Askew's data [12]

[2] Mass, wing span and area are obtained via personal communication with Professor G. Askew.

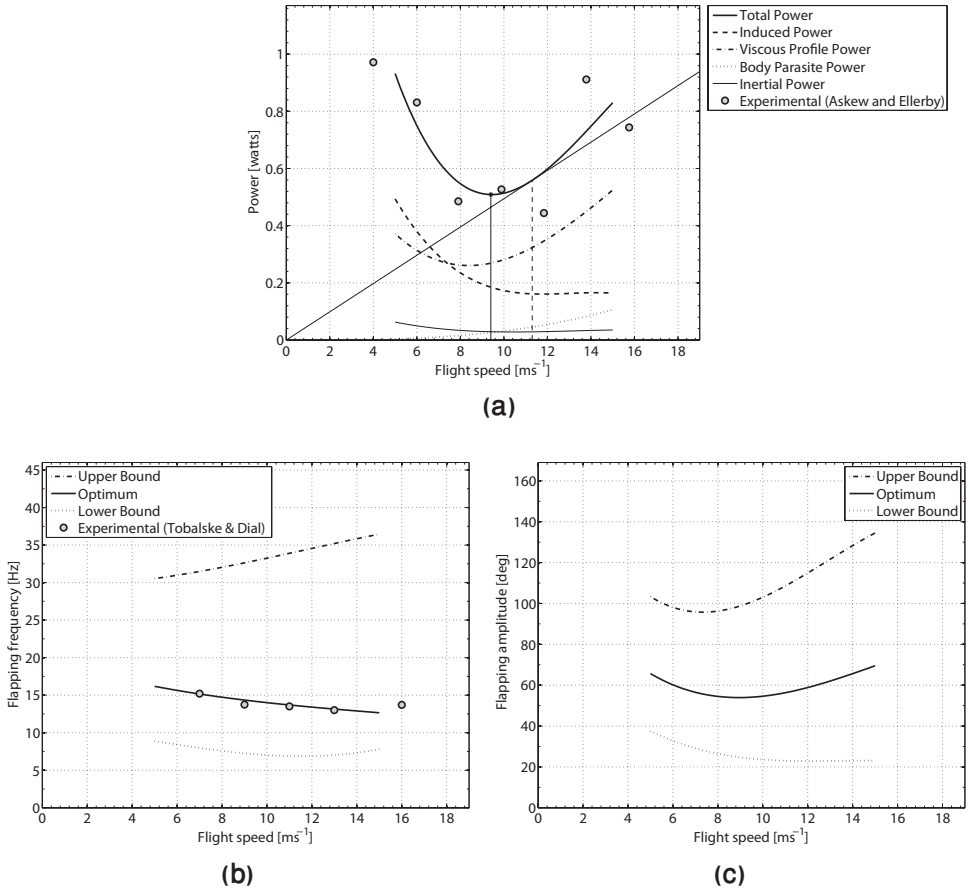

Figure 4: Flight kinematics and energetics as predicted by our model for a budgerigar (*Melopsittacus undulatus*). (a) Variation of total power and its sub-components as a function of flight speed compared with *in vitro* measurements [12], (b) flapping frequency and its 10% upper-lower bounds as a function of flight speed compared with wind tunnel data [13], (c) flapping amplitude and its 10% upper-lower bounds as a function of flight speed

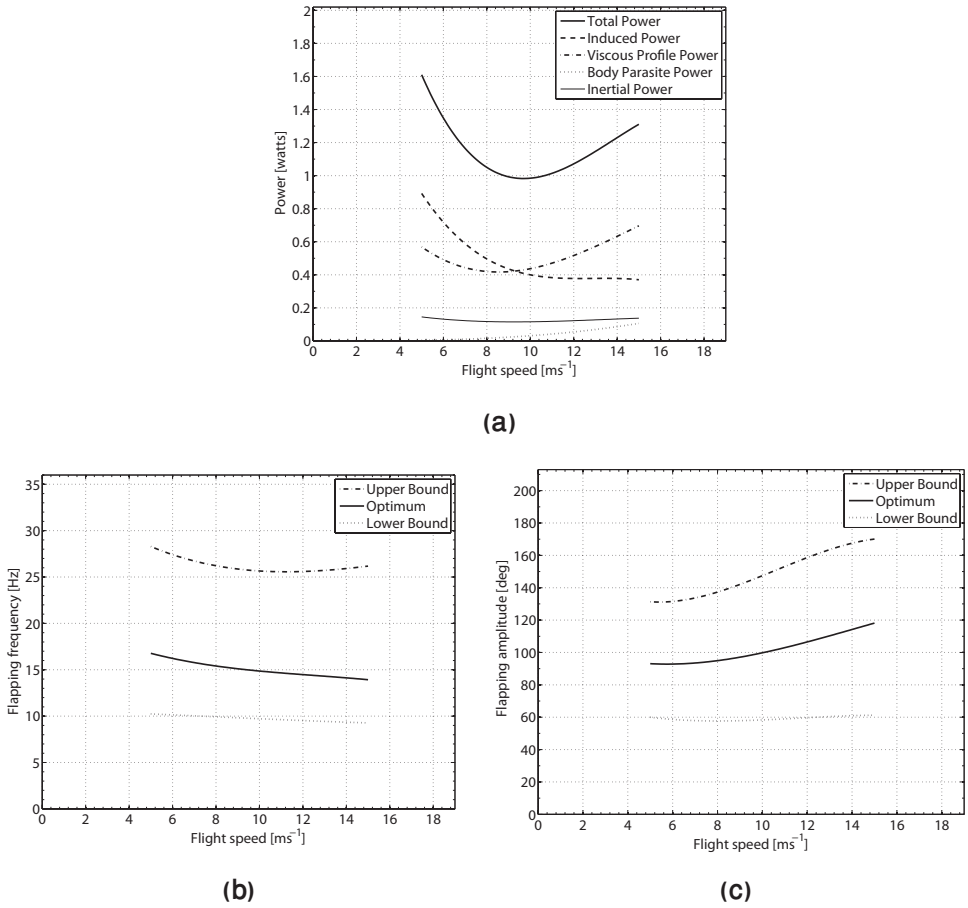

Figure 5: Ascending ($\theta = 15^\circ$ climb) flight kinematics and energetics predictions for a budgerigar (*Melopsittacus undulatus*). (a) Variation of total power and its sub-components as a function of flight speed, (b) flapping frequency and its 10% upper-lower bounds as a function of flight speed, (c) flapping amplitude and its 10% upper-lower bounds as a function of flight speed

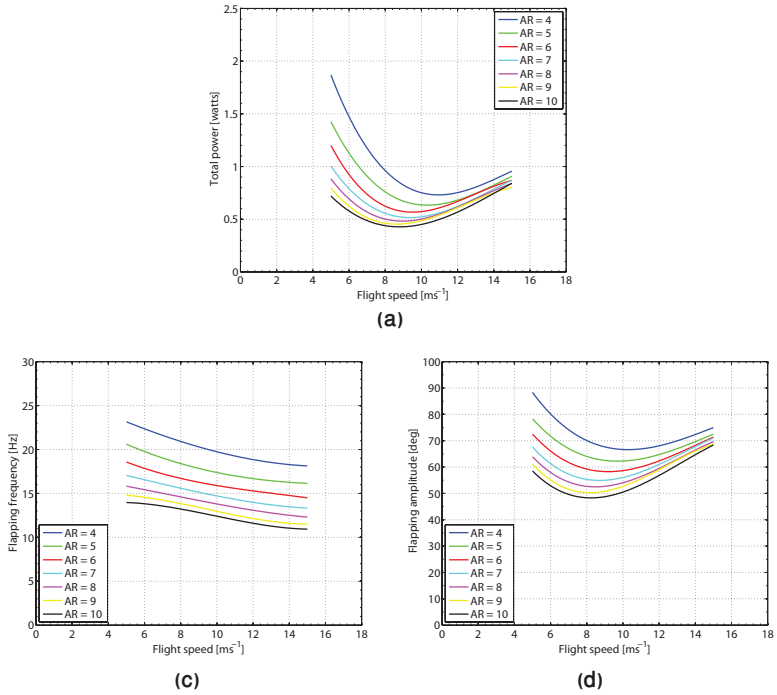

Figure 6: Energetics and kinematics variations for different aspect ratios, AR, while keeping wing planform area $S = 0.011\ m^2$ constant. (a) Variation of total power as a function of flight speed, (b) flapping frequency as a function of flight speed, (c) flapping amplitude as a function of flight speed.

of animals during takeoff and climb. By contrast, the wing-beat frequency has remained approximately constant in our predictions. This agrees with experimental observations of nearly constant flapping frequency across a range of flight conditions. The trade-off between frequency and amplitude is likely due to the greater dependence on frequency than amplitude in the inertial power computation ($P_{iner} \propto A^2 f^3$).

3.2 Parametric Study: MAV Preliminary Design

In this section we examine the preliminary design choices for an MAV with similar scale as the budgerigar – wing span $b = 0.3\ m$, and a mass of ($M = 45\ g$). The effect of aspect ratio variation on flight endurance and flight range as well as the energetics impact of constant-amplitude flapping and constant-frequency flapping will be the focus of our present study. The aspect ratio study focuses on two separate cases, namely, aspect ratio variations with constant-area and aspect ratio variations with constant span.

3.2.1 Parametric Study: Aspect Ratio Variation – Fixed Planform Area

First, we use the energetics model to examine the effect of wing aspect ratio (AR) on flight energetics, while maintaining a constant planform area, $S = 0.011\ m^2$ (the chord and span both change appropriately). The results (figure 6) show the variation of (a) total

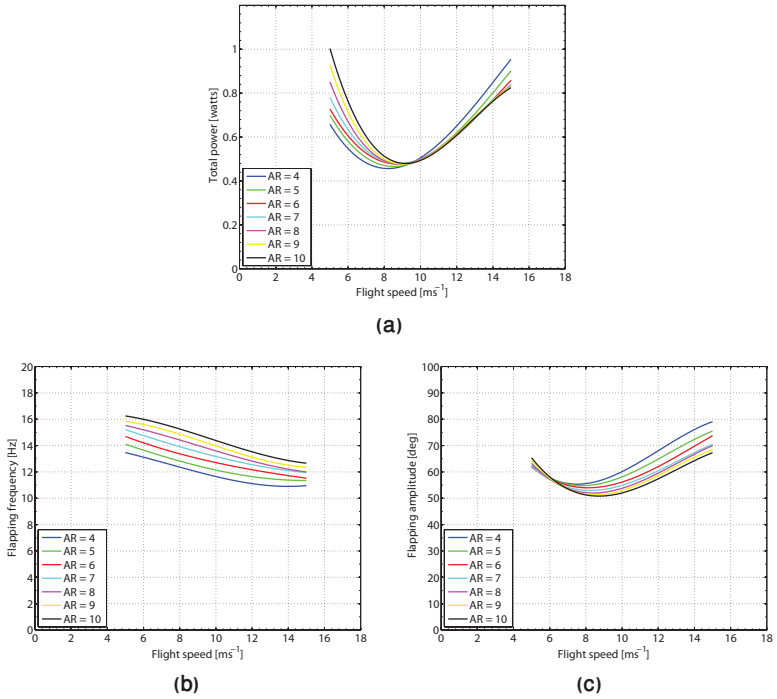

Figure 7: Energetics and kinematics variations for different aspect ratios, AR, while keeping wing span $b = 0.3\ m$ constant. (a) Variation of total power as a function of flight speed, (b) flapping frequency as a function of flight speed, (c) flapping amplitude as a function of flight speed.

power , (b) frequency and (c) amplitude as we change the wing AR while keeping planform area constant. These results demonstrate the advantage of choosing a higher aspect ratio wing if the planform area is to be held constant. Not only are power requirements reduced for constant-area, higher aspect ratio wings, the amplitude of flapping is also drastically less. This is critical in regions of the power curve where velocities are low.

3.2.2 Parametric Study: Aspect Ratio Variation – Fixed Span

In this section we examine the effect of wing aspect ratio (AR) variation while maintaining a constant span, $b = 0.3\ m$ (the area and thus wing loading change). The results (figure 7) show the variation of (a) total mechanical power , (b) frequency and (c) amplitude as we change the wing AR while keeping the span fixed. A fixed span constraint is relevant in MAV design due to the size constraints imposed in the MAV definition (for an MAV, span $\leq 15cm$). In addition, a fixed span constraint may also apply to some animals – specifically those that inhabit and navigate dense arboreal environments. The results of this study (figure 7) indicate that different aspect ratios are preferable depending on the overall mission of the vehicle. Because the span is fixed, a lower aspect ratio equates to a higher area and therefore a lower wing loading; hence, our results show that for lower speeds a lower aspect ratio is preferred, since wing loading is lower and therefore, induced

drag is reduced. On the other hand, as speed increases, the induced power benefit of a higher planform area is negated by the increased viscous drag; hence, as flight speed increases, higher aspect ratios are preferred. In the subsequent investigations we focus on the minimum power and maximum range flight conditions as a means to guide and assess aspect ratio selection. This investigation illustrates the impact of geometric design constraints (fixed area vs. fixed span) on MAV preliminary sizing and design.

3.2.3 Parametric Study: Fixed Amplitude or Frequency Flapping

There is a tradeoff between flapping mechanism complexity and vehicle weight. An engineered variable amplitude flapping mechanism will likely weigh more than a fixed amplitude flapping mechanism. We therefore explore the effects of constant frequency and constant amplitude flapping separately on the energetics of flapping flight. By knowing how particular flapping mechanism's constraints might impact the flight energetics, we can make informed decisions earlier in the design process about keeping certain flight flapping parameters constant.

In the extension of our bio-inspired MAV design study, we assess the impact of off-design performance due to fixing flapping amplitude or flapping frequency. The constant value of flapping frequency and amplitude are chosen based on the minimum power cruise condition. We then assess the off-design performance of the MAV by examining the fixed flapping kinematics in climbing flight. The effect of aspect ratio is examined in each of these cases. The following four cases are assessed during climbing flight at $\theta = 15°$:

- **Case 1**: 15 ° climbing flight, fixed area ($S = 0.011\ m^2$), $A = const. = 55$ °, frequency selected to minimize power.
- **Case 2**: 15 ° climbing flight, fixed area ($S = 0.011\ m^2$), $f = const. = 14\ Hz$, amplitude selected to minimize power.
- **Case 3**: 15 ° climbing flight, fixed span ($b = 0.3\ m$), $A = const. = 55$ °, frequency selected to minimize power.
- **Case 4**: 15 ° climbing flight, fixed span ($b = 0.3\ m$), $f = const. = 14\ Hz$, amplitude selected to minimize power.

Figure 8 shows the differences in power requirements for cases 1 and 2. Similarly, figure 9 demonstrates the same results for cases 3 and 4. The bar graphs illustrate the percent difference between the power computed between the optimal/baseline case (amplitude and frequency are both chosen to minimize flight power) and the constrained kinematics case – Case 1 through Case 4 (the amplitude or frequency is constrained, and the associated minimum power is found). During climbing flight, a prescribed frequency of $f = 14\ Hz$ is similar to the optimal flapping frequency for cruise and climbing flight (see figure4 and 5). Therefore with frequency fixed at $f = 14\ Hz$, we expect similar power requirements

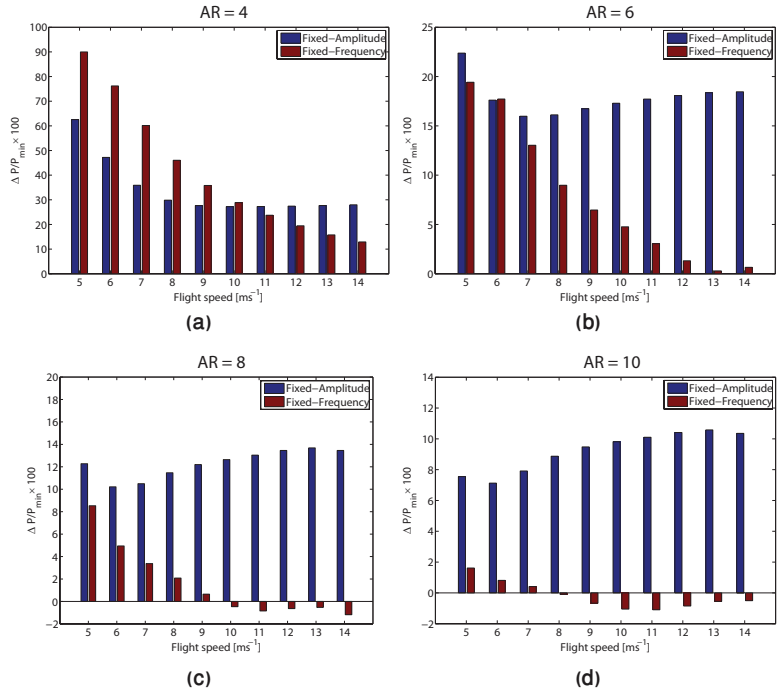

Figure 8: Comparing total power for different aspect ratios. The bar graphs show the percent difference between optimal energetics and fixed amplitude ($A = 55°$, maroon bars) as well as fixed frequency ($f = 14\ Hz$, blue bars). AR varies but area is fixed, $S = 0.011\ m^2$ (a) $AR = 4$, (b) $AR = 6$, (c) $AR = 8$, (d) $AR = 10$.

as in the unconstrained mode. Our computations show a very small interpolation error (approx. 2%).

From the trends shown in the constrained parameter flapping results (figure 8 - 9), it is clear that fixed frequency flapping is a superior energetics choice over fixed amplitude flapping for most aspect ratios. This result was expected based on the results of the energetics analysis of budgerigar (figures 4 and 5) that indicated little change in optimal flapping frequency with flight angle and flight speed.

The results in figure 8 show some deviation from the trend at lower aspect ratios. For $AR = 4$, a fixed amplitude flapping strategy was found to be a better option at lower flight speeds. For $AR = 4$, the results already demonstrated that the optimal frequency (figure 6–b) and amplitude (figure 6–c) are sufficiently different than the current wing-beat constraints (i.e. $f = 14\ Hz$ and $A = 55°$), implying a substantially off-design operating point.

For most cases explored in this study, fixed frequency appears to be a superior energetics choice. As a result, a fixed frequency is selected for further exploration. We recalculate the energetics results for level flight shown in (figures 6 and 7) with a fixed frequency of $f = 14\ Hz$. The role of aspect ratio on energetics for this fixed flapping frequency case is examined in figures 10 and 11.

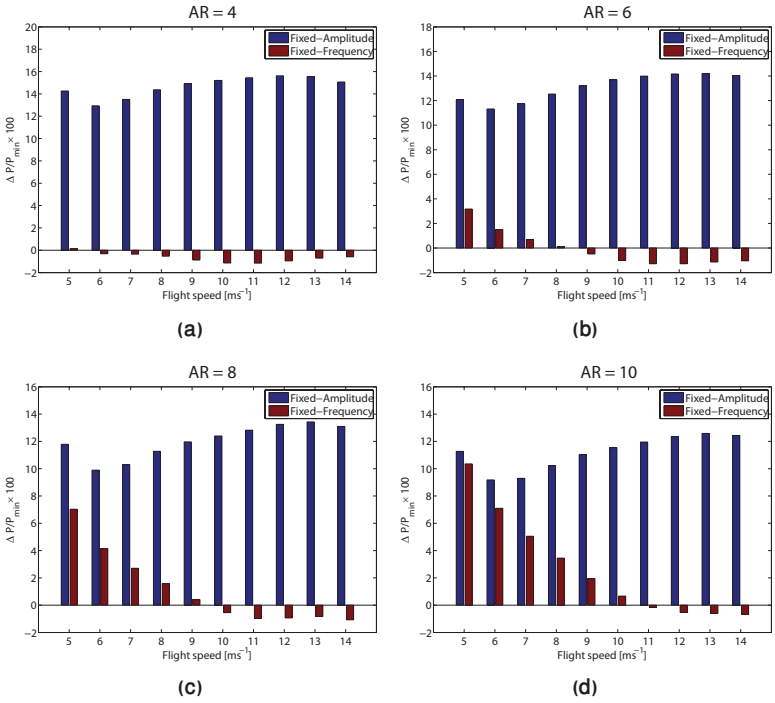

Figure 9: Comparing total power for different aspect ratios. The bar graphs show the percent difference between optimal energetics and fixed amplitude ($A = 55°$, maroon bars) as well as fixed frequency ($f = 14\ Hz$, blue bars). AR varies but span is fixed at $b = 0.3\ m$ (a) $AR = 4$, (b) $AR = 6$, (c) $AR = 8$, (d) $AR = 10$.

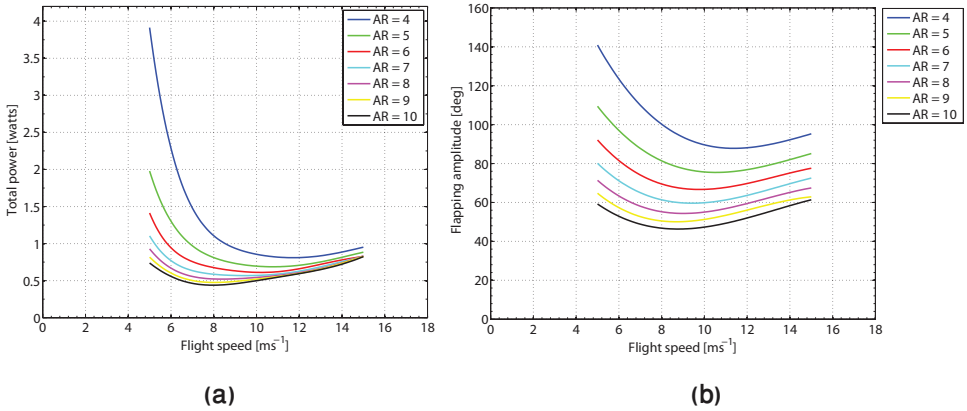

Figure 10: Energetics and kinematics variations for different aspect ratios, AR, while keeping wing area constant ($S = 0.011\ m^2$), and constant frequency $f = 14\ Hz$ flapping strategy. (a) Variation of total power as a function of flight speed, (b) flapping amplitude as a function of flight speed.

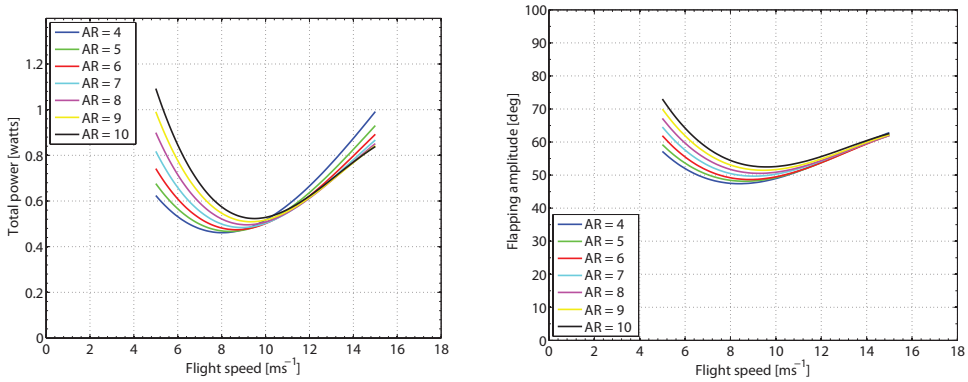

Figure 11: Energetics and kinematics variations for different aspect ratios, AR, for a fixed span, $b = 0.3m$, and constant frequency $f = 14\ Hz$ flapping strategy. (a) Variation of total power as a function of flight speed, (b) flapping amplitude as a function of flight speed.

The aspect ratio, wing area (or wing span), flapping frequency and flapping amplitude can be manipulated and selected based on the results thus far. Depending on the specific mission of an MAV, different design choices may be made. For example, a long endurance MAV requires minimum power (P_{mp} is the minimum point of the power curve in figure 10–a or 11–a) whereas maximizing vehicle range requires minimizing the maximum range power (maximum range power, P_{mr}, is defined by a line that passes through the origin and is tangent to the power curve at the location where $P = P_{mr}$). We extracted this data from figures 10 and 11 and have summarized the results in tables 3 and 4 respectively.

Depending on the design objectives (fixed/prescribed area or fixed/prescribed span), results like those shown in tables 3 and 4, can be used to guide initial design decisions. For example, highest endurance (lowest P_{mp}) for a fixed span of 0.3 m occurs for $AR = 4$, whereas, for an unconstrained span, the best aspect ratio choice is the highest aspect ratio considered, $AR = 10$.

The maximum range per unit energy, R_{max} in $(m/joule)$, is predicted from our results using:

$$R_{max} = \frac{\Delta Distance}{\Delta E} = \frac{V_{mr} \cdot \Delta t}{\Delta E} = \frac{V_{mr}}{P_{mr}} \tag{1}$$

The calculated R_{max} are shown in tables 3 and 4. By using the above metric, the distance travelled per joule is maximized for an aspect ratio $AR = 7$ when the span is held constant at 0.3 m. Similarly, for a fixed planform area, ($S = 0.011\ m^2$), the maximum distance per joule is achieved when the aspect ratio is maximum, in this study this corresponds to $AR = 10$. The optimal aspect ratio for this MAV design is different depending on the design constraints. If a maximum span is prescribed, a lower aspect ratio maximizes range because of the increased planform area and reduced wing loading. On the other hand, if the span is unconstrained, and wing area is held constant, the results indicate a

	$AR=4$	$AR=5$	$AR=6$	$AR=7$	$AR=8$	$AR=9$	$AR=10$
P_{mp} (watts)	0.810	0.687	0.611	0.568	0.521	0.476	0.439
P_{mr} (watts)	0.898	0.758	0.666	0.633	0.618	0.603	0.589
V_{mr} (m/s)	14.2	13.1	12.1	12.1	12.2	12.1	11.9
R_{max} (m/J)	15.8	17.3	18.2	19.1	19.8	20.1	20.2

Table 3: Level flight, minimum power, P_{mp}, maximum range power P_{mr}, maximum range velocity V_{mr} and maximum range per unit energy R_{max}, for different ARs while keeping area fixed at $S = 0.011\ m^2$. Numerical data extracted from figure 10 for a fixed frequency mechanism with a constant frequency of $f = 14\ Hz$.

	$AR=4$	$AR=5$	$AR=6$	$AR=7$	$AR=8$	$AR=9$	$AR=10$
P_{mp} (watts)	0.461	0.467	0.474	0.484	0.496	0.509	0.523
P_{mr} (watts)	0.512	0.515	0.524	0.532	0.539	0.555	0.568
V_{mr} (m/s)	9.9	10.2	10.5	10.7	10.8	11.0	11.1
R_{max} (m/J)	19.3	19.8	20.0	20.1	20.0	19.8	19.5

Table 4: Level flight, minimum power, P_{mp}, maximum range power P_{mr}, maximum range velocity V_{mr} and maximum range per unit energy R_{max}, for different ARs while keeping span fixed at $b = 0.3m$. Numerical data extracted from figure 11 for a fixed frequency mechanism with a constant frequency of $f = 14\ Hz$.

higher aspect ratio is favorable for reducing the induced drag. While there is evidence that changing aspect ratio will improve flight endurance and range, we do caution that these parameters may also strongly be influenced by other considerations including wing root moments, flight environment and biological/engineering material selection constraints.

4 CONCLUSIONS

Our novel energetics model has generated the first computationally predicted, strongly linked, relationship between power requirements and wing-beat kinematics. Whether it is used in biological predictions of power and kinematics or engineering MAV design, this computational model is capable of efficiently and robustly exploring the design space. We presented results for a budgerigar. Based on this flier, we presented several parametric studies for preliminary design decisions for a comparable sized MAV. We investigated the off-design performance of this same exemplar bio-inspired MAV design. Different Aspect Ratios (ARs) were explored for level and climbing flight. By investigating constant amplitude and constant frequency flapping motions we were able to conclude that in the majority of cases, fixing the flapping frequency and modulating the wing-beat amplitude is a better choice than fixing the amplitude and modulating the frequency. Finally, depending on the geometrical design constraints (whether span or area is constrained) and the objective (maximum range or maximum endurance) of the bio-inspired MAV, we were able to show that different aspect ratios should be chosen. While this example illustrates a exploration of a single bio-inspired MAV, we expect our energetics model to have broad applicability across a range of MAV designs.

REFERENCES

[1] Shyy, W., Berg, M. and Ljungqvist, D., "Flapping and Flexible Wings for Biological and Micro Air Vehicles, *Progress in Aerospace Sciences*, Vol. 35, 1999, pp. 155-205.

[2] Norberg U. M., "Vertebrate Flight," *Berlin: Springer Verlag*, 1991.

[3] Pennycuick C. J., "Power requirements for horizontal flight in the pigeon Columba livia," *J. Exp. Biol.*, Vol. 49, 1968, pp. 527-555.

[4] Pennycuick C. J. "Mechanics of flight," *Avian Biology Vol. 5*, eds D. S. Farner, J. R. King and K. C. Parkes (Academic Press), Vol. 5, pp. 1-75.

[5] Rayner J. M. V. (1979c) A vortex theory of animal flight. Part 2. The forward flight of birds. *J. Fluid Mech*, Vol. 91, No 4, 1979, pp. 731-763.

[6] Videler J. J., "Avian Flight," *Oxford University Press*, 2005.

[7] Pennycuick C. J., "Modelling the flying bird," *Elsevier Ltd*, 2008.

[8] Salehipour, H., Willis, D.J., "A coupled kinematics and energetics model for flapping flight," *48th AIAA Aerospace Sciences Meeting and Exhibit*, Orlando, Florida, January 2010, AIAA-2010-1229.

[9] Hall, K. C., Pigott, S. A. and Hall, S. R.,"Power requirements for large-amplitude flapping flight," *J. Aircraft*, Vol. 35, pp. 352-361.

[10] Salehipour, H, "A Fast Low-Fidelity Computational Model: Examining Flapping Flight Energetics in Nature and Engineering," *Master's thesis*, In prep., UML, 2010.

[11] Pennycuick, C. J.,"On the reconstruction of pterosaurs and their manner of flight, with notes on vortex wakes," *Biol. Rev.*, Vol. 63, 1988, pp. 299-331.

[12] Askew, G. N. and Ellerby, D. G., "The mechanical power requirements of avian flight," *Biol. Lett.*, Vol. 3, 2007, pp. 445-448.

[13] Tobalske, B. W. and Dial, K. P., "NEUROMUSCULAR CONTROL AND KINEMATICS OF INTERMITTENT FLIGHT IN BUDGERIGARS (MELOPSITTACUS UNDULATUS)," *J. exp. Biol.*, Vol. 187, 1994,pp. 1-18.

[14] Tobalske, B. W., Warrick, D. R., Clark, C. J., Powers, D. R., Hedrick, T. L., Hyder, G. A. and Biewener, A. A., "Three-dimensional kinematics of hummingbird flight," *J. Exp. Biol.*, Vol. 210, 2007, pp. 2368-2382.